

Evaluation of Degradation Models for High Strength *p*-Aramid Fibres Used in Body Armour

K.D. Rice¹, A. Engelbrecht-Wiggans², E. Guigues¹, and A.L. Forster¹

¹National Institute of Standards and Technology, 100 Bureau Drive, Gaithersburg, MD, USA
kirk.rice@nist.gov

²Theiss Research

Abstract. To improve the reliability and design of armour, it is imperative to understand the failure modes and the degradation rates of the materials used in armour. Despite the best efforts of manufacturers, some vulnerability of armour materials to ageing due hydrolytic or oxidative environments is expected and may result in the degradation of material properties such as tensile strength. In this work, *p*-aramid yarns from two manufacturers were exposed to environmental conditions of various fixed temperature and humidity combinations. The maximum temperature and humidity condition was 70 °C, 76 % RH, to avoid introducing degradation mechanisms unlikely to be seen in use. Tensile tests were performed on samples extracted at several different timepoints over the course of at least one year to determine degradation in ultimate tensile strength and failure strain as a function of time, temperature, and humidity. These materials were found to be generally resistant to degradation at most conditions, only showing changes of less than 10 % at the highest temperature and humidity conditions.

1. INTRODUCTION

The National Institute of Standards and Technology (NIST) has a longstanding commitment to ensuring the safety of body armour used by law enforcement officers in the United States through a research program addressing the long-term stability of high strength fibres used in body armour. Prior work [1]–[3] has focused on the field failure of a body armour made from the material poly(*p*-phenylene-2,6-benzobisoxazole), or PBO, which led to a major revision to the National Institute of Justice’s (NIJ) body armour standard in 2008 [4]. Since the release of this revised standard, work has continued at NIST to examine mechanisms of ageing in other commonly used fibres such as ultra-high molar mass polyethylene [5] and poly(*p*-phenylene terephthalamide), or PPTA, commonly known as aramid. This work will focus on the long-term stability of aramid yarns manufactured by two different companies after both exposure to conditions of elevated temperature and also to conditions of elevated temperature and humidity.

The commercialization of aramid fibres ushered in the era of modern body armour. In the early 1970s, NIJ partnered with the Department of Defense (DOD) to develop and pilot lightweight protective armour based on aramids, and by 1975, the first officer had been saved through this program [6]. To date, over 3100 law enforcement officers’ lives have been saved by wearing body armour [7]. Guidelines for the replacement of law enforcement officers’ body armour have been the focus of several historical efforts. Two studies are commonly cited, one undertaken by DuPont in the 1980s [8], and one by NIST (then the National Bureau of Standards, NBS) which was published in 1986 [9]. The DuPont study showed a reduction in ballistic performance of heavily used aramid armour after 3 to 5 years of use, however, that reduction in ballistic performance was better correlated to the heavy use than the age of the armour [8]. The NBS study examined 24 aramid armours of the same design that had been in use in various conditions and climates for 10 years [9]. The author of the NBS study concluded that aramid armour stored in climate controlled conditions would maintain its ballistic resistance for at least 10 years, however the extremely limited sample size in this study makes it difficult to draw meaningful and broad conclusions about aramid armour lifetime [9]. DuPont recommended a 5-year service life as a result of their study [8], which remains a common service life for armour today. Both studies were more focused on ballistic performance of aramid armour, and less on potential mechanisms of environmental degradation to the aramid polymer, however other studies have addressed the stability of aramids from the standpoint of fundamental material properties.

Aramid is a condensation polymer and is well known to be susceptible to degradation by chain scission through a hydrolysis reaction that attacks the amide linkage between phenylene rings, which is generally expected to be catalysed by an acid or base [1], [10]–[14]. A simple scheme for this reaction is given in Figure 1. Several authors [10]–[20] have examined the effect of exposure to environments of elevated temperature, humidity, light, pH, or some combination thereof on the physical and chemical properties of PPTA fibres. For the purposes of comparison with this study, the previous work of the most interest focuses on the lower temperature thermal (temperatures below 100 °C) and hydrolytic

stability of PPTA. Several researchers [11], [12], [14], [15], [17], [18] performed studies in which PPTA fibres were immersed in solutions to examine hydrolysis, sometimes with non-neutral pH, while others [10], [13] used exposure to elevated conditions of temperature and relative humidity. The latter describes the approach taken in this study because it best mimics a common hydrolytic exposure mechanism encountered in body armour, where water vapour moves through the armour panel structure, even though the ballistic material might be shielded from contact with liquid water by a waterproof cover. Despite precautions taken to prevent liquid water from contacting the ballistic material, in practice this can still occur either due to deficiencies in the waterproof barrier, or due to vapour permeability of the cover with subsequent condensation of the water vapour inside the armour panel, or perhaps due to the presence of water adsorbed to the surfaces of the ballistic material initially. The hydrolysis mechanism described is valid, regardless of the state of the water.

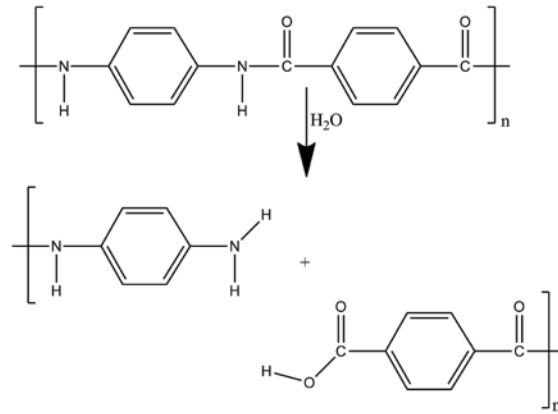


Figure 1. Schematic of PPTA hydrolysis mechanism.

The strength retention of aramid yarns after exposure to thermooxidative or hydrolytic conditions has been the focus of several previous studies. Arrieta and co-authors recently [10] exposed blends of PPTA-PBI to hydrolytic conditions of 50 °C, 60 °C, and 70 °C at 50 % relative humidity (RH) and 60 % RH up to 31 days, and observed a loss of approximately half of the original tensile strength of the yarn at the most severe condition (70 °C, 60 % RH). These authors also propose a mathematical model for hydrolysis of aramid based on molecular spectroscopy, which will not be discussed further here, but is an area of interest for future work. In research published in 1989, Auerbach [13] exposed PPTA fibres to conditions of elevated temperature ranging from 130 °C to 170 °C and humidity ranging from 0 % RH to 90 % RH up to 3 months, and calculated rate constants for degradation. Auerbach proposes two equations, one for thermooxidative degradation (in the absence of humidity) and one for hydrolytic degradation (with humidity). Springer [12] and co-authors build upon Auerbach's work and propose a model of tensile strength evolution for aramid yarns, which will be further examined below. The models proposed by Auerbach and Springer will be examined and fitted to the strength data for aramid yarns that were exposed to various combinations of humidity and temperature in the laboratory, and compared to a simple power law decay model.

Mechanical properties are of special interest because there is a relationship between the material properties of the yarn and the ballistic-resistance of optimised armour made from the yarn. The ballistic-resistance of the hypothetical armour is described in terms of V_{50} , which is the velocity at which half of the projectiles are expected to perforate the armour. Cunniff's landmark paper [21] relating V_{50} to material properties described two dimensionless ratios, $\frac{V_{50}}{(U^*)^{1/3}}$ and $\Gamma_0 = \frac{A_d A_p}{m_p}$, where A_d is the armour system areal density, A_p is the projectile presented area, m_p is the projectile mass, and $U^* = \frac{\sigma \varepsilon}{2\rho} \sqrt{\frac{E}{\rho}}$, where σ is the fibre ultimate axial tensile strength, ε is the fibre ultimate tensile strain, ρ is the fibre density, and E is the fibre modulus.

Furthermore, these two ratios are related through a function shown in Equation 1.

$$\Phi\left(\frac{V_{50}}{(U^*)^{1/3}}, \Gamma_0\right) = 0 \quad (1)$$

Cunniff [21] empirically determined this function, however this analysis was extended by Phoenix and Porwal [22], who developed a membrane model in which they determined this function, given in Equation 2.

$$\frac{V_{50}}{(U^*)^{1/3}} = f(\Gamma_0) \quad (2)$$

The resulting functional form is shown in Equation 3,

$$\frac{V_{50}}{(U^*)^{1/3}} = \frac{2^{1/3} \varepsilon^{1/12} (1 + \theta^2 \Gamma_0)}{K_{\max}^{3/4}}, \quad (3)$$

where θ is an adjustment parameter, typically between 1.25 and 1.35, to account for various factors such as plastic projectile nose deformation, fabric wraparound, etc., and K_{\max} is given by

$$K_{\max} = \exp \left\{ -\frac{4\theta^2 \Gamma_0 (\psi_{\max}^2 - 1)}{3(1 + \theta^2 \Gamma_0)} \right\} \psi_{\max}^{1/3} \left[\frac{\sqrt{\frac{\psi_{\max}}{\varepsilon}} (\psi_{\max} - 1)}{\ln \left\{ 1 + \sqrt{\frac{\psi_{\max}}{\varepsilon}} (\psi_{\max} - 1) \right\}} \right]^{2/3}, \quad (4)$$

where

$$\psi_{\max} \approx \sqrt{\frac{1 + \theta^2 \Gamma_0}{2\theta^2 \Gamma_0}}. \quad (5)$$

The derivations of these relationships involve simplifying assumptions; however, they provide a convenient means for estimating how changes in some parameters might affect armour performance. The parameters θ and Γ_0 can be assumed to remain constant with ageing as they only consider details of the ballistic impact. However, ageing has the potential to change the ultimate tensile strength, σ , the failure strain, ε , and the fibre density, ρ . In some systems only the tensile strength changes. In these cases ψ_{\max} is constant, K_{\max} is constant, and thus $\frac{V_{50}}{(U^*)^{1/3}}$ is also constant. From this information we can determine that

$$\frac{V_{50 \text{ aged}}}{V_{50 \text{ new}}} = \left(\frac{U^*_{\text{aged}}}{U^*_{\text{new}}} \right)^{1/3} = \left(\frac{\sigma_{\text{aged}} \sqrt{\frac{E_{\text{aged}}}{E_{\text{new}}}}}{\sigma_{\text{new}} \sqrt{\frac{E_{\text{aged}}}{E_{\text{new}}}}} \right)^{1/3} = \sqrt{\frac{\sigma_{\text{aged}}}{\sigma_{\text{new}}}}. \quad (6)$$

In the case where the failure strain and the ultimate stress both change, but the material remains linear, it can be shown that

$$\frac{V_{50 \text{ aged}}}{V_{50 \text{ new}}} = \left(\frac{U^*_{\text{aged}}}{U^*_{\text{new}}} \right)^{1/3} \left(\frac{K_{\text{new}}}{K_{\text{aged}}} \right)^{3/4} \left(\frac{\varepsilon_{\text{aged}}}{\varepsilon_{\text{new}}} \right)^{1/12} \quad (7)$$

and

$$\frac{V_{50 \text{ aged}}}{V_{50 \text{ new}}} = \left(\frac{\sigma_{\text{aged}}}{\sigma_{\text{new}}} \right)^{1/2} \left(\frac{\varepsilon_{\text{aged}}}{\varepsilon_{\text{new}}} \right)^{1/2} \left(\frac{\ln \left\{ 1 + \sqrt{\frac{\psi_{\max}}{\varepsilon_{\text{aged}}}} (\psi_{\max} - 1) \right\}}{\ln \left\{ 1 + \sqrt{\frac{\psi_{\max}}{\varepsilon_{\text{new}}}} (\psi_{\max} - 1) \right\}} \right)^{1/2}. \quad (8)$$

2. EXPERIMENTAL

2.1 Materials and ageing conditions

Aramid yarns from two different manufacturers were used in these experiments. Aramid A was nominally 93 tex, and Aramid B was nominally 167 tex. All yarns were wound onto smooth plastic

spools and placed into chambers for ageing experiments. Preliminary testing was performed with a number of different spool substrate materials, including glass, to determine whether any interactions between the aramid yarns and the spool substrate would affect results. Findings indicated that there were no discernible differences in the IR spectra of the yarn fibres between the plastic spools and the glass spools, so smooth plastic spools were used. Conditions noted as “dry” were generated by putting the yarns inside of desiccators filled with calcium sulphate desiccant inside of an oven at either 25 °C, 43 °C, 55 °C, or 70 °C. Conditions noted as “humid” were generated by putting yarns in humidity chambers controlled to 25 °C, 27 % RH; 43 °C, 41 % RH; 55 °C, 60 % RH; or 70 °C, 76 % RH. These conditions were selected to all result in a 3 % moisture content in the yarn, as determined by previous moisture sorption studies (not reported here due to space limitations.) Prior to conducting extractions of yarns for testing throughout the ageing experiments, all chambers were returned to room temperature and humidity, when applicable, by first reducing the humidity of the chamber to a low humidity (10 % RH to 15 % RH), and then reducing the temperature to 25 °C. All chambers provided control to ± 1 °C in temperature and ± 5 % RH.

2.2 Strength measurements

Tensile testing on exposed PPTA fibres was carried out in accordance with ASTM D2256-02, “Standard Test Method for Tensile Properties of Yarn by the Single-Strand Method”, using an Instron¹ Model 5582 screw-driven universal frame equipped with a 1 kN load cell, and pneumatic yarn and cord grips (Instron model 2714-006). Strain measurements were taken with an Instron non-contacting Type 3 video extensometer in conjunction with black foam markers placed approximately 2.5 cm apart in the gage section of the yarn. Grip separation was 7.9 cm and cross head speed was 0.38 mm/s. Each yarn was nominally 40 cm long and was given 64 twists on a custom-designed yarn twisting device. The standard uncertainty in tensile strength and breaking strain are approximately ± 3 %. At least 14 samples were tested for each data set.

3. RESULTS AND DISCUSSION

2.3 Effect of ageing on tensile strength

Yarn samples of Aramid A and Aramid B were exposed to conditions as described in Section 2.1. Yarn test specimens were periodically taken from the spools and the tensile strength and elongation at break were determined. Elongation at break was relatively invariant over the course of the study and will not be discussed herein due to space limitations. A summary of ultimate tensile strengths for the different ageing conditions at initial time and the end of the ageing experiment are presented in Table 1.

A few observations can be drawn from a simple examination of the values of the initial and final tensile strengths of the aged samples. Unsurprisingly, the lower temperature and lower relative humidity conditions cause little change in the tensile strength for either aramid, especially when the standard deviation is considered. At 25 °C the final samples are always greater than 90 % of the initial mean, so there is less than 10 % degradation in strength. Furthermore, both aramids had no statistically significant differences (using the Student’s t-test at the 0.01 significance level) between samples at any of the extraction times both 25 °C conditions (with and without humidity).

Some samples appeared to increase in strength, most notably the 70 °C, 0 % RH condition for aramid B. However, when this sample’s mean tensile strength is compared to that of the sample extracted after week 1 (mean tensile strength of 2.78 GPa with a standard deviation of 0.15) there is no statistically significant difference. This apparent increase in tensile strength could be explained if the ageing study functioned as a heat treatment for the aramid B fibres. Heat treatment history of both samples was not provided, but it is possible that aramid A was heat treated and aramid B was not. A further explanation for why these samples appeared to increase in strength will be investigated for future work. 

A Student’s t-test was used to assess differences in the tensile strength between the different extraction times and ageing conditions for all samples. In general, degradation only appears to occur at high temperatures. For aramid A, both 70 °C conditions (with and without humidity) showed a statistically significant difference (0.05 significance level) from the initial starting condition. This indicates that the aramid A is susceptible to degradation at high temperatures, even without the presence 

¹ Certain commercial materials and equipment are identified in this paper to specify adequately the experimental procedure. In no case does such identification imply recommendation or endorsement by the National Institute of Standards and Technology, nor does it necessarily imply that the product is the best available for the purpose.

of humidity. However, aramid B only appears susceptible to degradation at conditions of high temperature and high humidity, with the only statistically significant difference in mean tensile strength observed at the 70 °C, 76 % RH condition.

Table 1. Mean ultimate tensile strength for initial (denoted as $\bar{\sigma}_b^i$) and longest ageing time (denoted as $\bar{\sigma}_b$), in GPa for aramid A and aramid B. All values are the mean of at least 14 samples. Standard deviations are presented in parentheses below the value. Ageing times are given in days. Statistically significant differences between initial and final tensile strength are denoted by bold text.

	Aramid A		Aramid B	
	$\bar{\sigma}_b$ (std)	ageing duration	$\bar{\sigma}_b$ (std)	ageing duration
Units	GPa	d	GPa	d
$\bar{\sigma}_b^i$ (std), GPa	3.14 (0.19)	0	2.52 (0.20)	0
25 °C, 0 % RH	3.13 (0.20)	280	2.55 (0.12)	280
25 °C, 27 % RH	3.17 (0.12)	525	2.45 (0.22)	525
43 °C, 0 % RH	3.15 (0.14)	280	2.54 (0.21)	280
43 °C, 41 % RH	3.22 (0.13)	525	2.52 (0.17)	525
55 °C, 0 % RH	3.21 (0.18)	280	2.58 (0.18)	280
55 °C, 60 % RH	3.19 (0.23)	434	2.44 (0.10)	525
70 °C, 0 % RH	2.87 (0.14)	280	2.77 (0.12)	280
76 °C, 76 % RH	2.91 (0.18)	280	2.18 (0.23)	280

2.4 Models used to describe aramid degradation

2.4.1 Auerbach's model

Auerbach [13] performed an analysis of the chemical kinetics of aramid degradation in a paper published in 1989. This work was performed in the context of predicting aramid and nylon parachute lifetimes, so in addition to temperature and humidity exposure, yarns were tightly knotted to mimic the folding within the parachutes. Auerbach successfully modelled the degradation of aramid with an empirical second-order rate relationship. Two primary degradation mechanisms were found. At low humidity, a thermooxidative degradation mechanism dominates. At high humidity, Auerbach found that a “moisture-induced” mechanism dominated, presumably hydrolysis. Auerbach's formula is given in Equation 9, where $\sigma_b(t)$ is the ultimate tensile strength at a given ageing time (t), k is a rate constant, t is time, and σ_b^i is the initial ultimate tensile strength.

$$\sigma_b(t) = \frac{1}{kt + \frac{1}{\sigma_b^i}} \quad (9)$$

Based on this analysis, Auerbach states that “less than 10 % degradation will take place at 25 °C” for aramid yarns [13], as was observed in this study.

2.4.2 Springer's model

Springer [12] and co-authors also examined the chemical kinetics of aramid degradation in a paper published in 1998. In this paper, poly(terephthalamides) were also studied, and the effect of very harsh conditions such as acid, base, and salt solutions were also examined, but only the elevated temperature and humidity exposures will be considered for the purposes of this publication. Springer and co-authors

applied Auerbach's model to their ageing results, and found that it did not fit their data. Instead of two separate chemical mechanisms, Springer and co-authors propose a single degradation model with two different "processes" occurring simultaneously. The equation for their model is presented in Equation 10 below, where $\sigma_b(t)$ is the ultimate tensile strength at a given ageing time (t), t is time, τ_1 and τ_2 are decay time constants, σ_b^i is the initial ultimate tensile strength, and a_1 and a_2 are weighting factors for the relative proportions of the decay processes. As shown in Equation 11, these weighting factors must sum to 1.

$$\sigma_b(t) = \sigma_b^i \left[a_1 \exp \left\{ -\frac{t}{\tau_1} \right\} + a_2 \exp \left\{ -\frac{t}{\tau_2} \right\} \right] \quad (10)$$

$$a_1 + a_2 = 1 \quad (11)$$

Springer [12] and co-authors do not attribute these two processes to any specific chemical mechanisms, but postulate some potential explanations for the observed behaviour. They consider that the observed phenomenon may be attributed to the shell/core structure of the fibre, reactions in crystalline regions vs. amorphous regions of the polymer, or differing stress states in the polymer (e.g., slack vs. tight tie molecules).

2.4.3 Power law

In addition to the empirically derived models presented above, a simple power law model was also fit to the ageing data. The equation for this model is presented in Equation 12, where $\sigma_b(t)$ is the ultimate tensile strength at a given ageing time (t), k is a rate constant, t is time, ρ is an exponential fitting parameter on time, and σ_b^i is the initial ultimate tensile strength.

$$\sigma_b(t) = \sigma_b^i - kt^\rho \quad (12)$$

By using only one rate constant, the power law model implies a single degradation process is occurring in the system. In Table 2, a list of the parameters used in the various models is presented.

Table 2. Values of parameters used in the Auerbach, Springer, and Power law models.

Auerbach parameter values

	Aramid A		Aramid B	
	σ_b^i (GPa)	k (1/GPa d)	σ_b^i (GPa)	k (1/GPa d)
25 °C, 0 % RH	3.254	5.374E-12	2.565	2.13E-12
25 °C, 27 % RH	3.108	1.542E-11	2.734	0.00E+00
70 °C, 0 % RH	3.139	7.392E-15	2.562	1.30E-14
70 °C, 76 % RH	3.113	9.336E-12	2.307	2.39E-11

Springer parameter values

	Aramid A				Aramid B			
	σ_b^i (GPa)	a_1	τ_1 (d)	τ_2 (d)	σ_b^i (GPa)	a_1	τ_1 (d)	τ_2 (d)
25 °C, 0 % RH	3.278	1.0000	9.92E+03	9.92E+03	3.060	0.8425	2.30E+04	1.36E-03
25 °C, 27 % RH	3.254	1.0000	2.64E+03	3.13E-03	2.743	1.0000	4.28E+13	
70 °C, 0 % RH	3.141	1.0000	4.14E+04	7.81E-04	2.564	1.0000	3.03E+04	6.35E-03
70 °C, 76 % RH	3.200	1.0000	4.54E+03	6.52E-03	2.439	1.0000	2.26E+03	6.56E-03

Power-law parameter values

	Aramid A			Aramid B		
	σ_b^i (GPa)	k (1/d $^\rho$)	ρ	σ_b^i (GPa)	k (1/d $^\rho$)	ρ
25 °C, 0 % RH	3.289	1.55E+04	1.572	2.561	3.59E+05	-2.536
25 °C, 27 % RH	3.294	3.30E+06	0.823	2.739	6.56E-11	-18.660
70 °C, 0 % RH	3.281	1.49E+08	0.044	2.554	1.22E+07	-0.981
70 °C, 76 % RH	3.193	8.46E+03	1.777	2.507	2.21E+07	0.490

2.4.4 Application of the models and goodness of fit

The three different models were applied to the ultimate tensile strength data generated in this study and fitting parameters optimised through least squares regression. As described previously, significant decreases in the tensile strength after long ageing times, some almost 2 years, were only observed for the 70 °C, dry, and the 70 °C, 76 % RH conditions for aramid A, and the 70 °C, 76 % RH conditions for aramid B. Since the greatest change was observed at the highest temperature, the examination of the models will be focused on 70 °C, dry and 70 °C, 76 % RH conditions for both aramids. The 25 °C, dry and 25 °C, 27 % RH data are also included in this analysis for comparison. Figure 2 shows the change in the mean ultimate tensile strength over ageing time for aramid A under these conditions, and Figure 3 shows the change in ultimate tensile strength over ageing time for aramid B. Curves representing the three different models are overlaid on the graphs. Goodness of fit for the models was assessed using r-squared values, which are presented in Table 3.

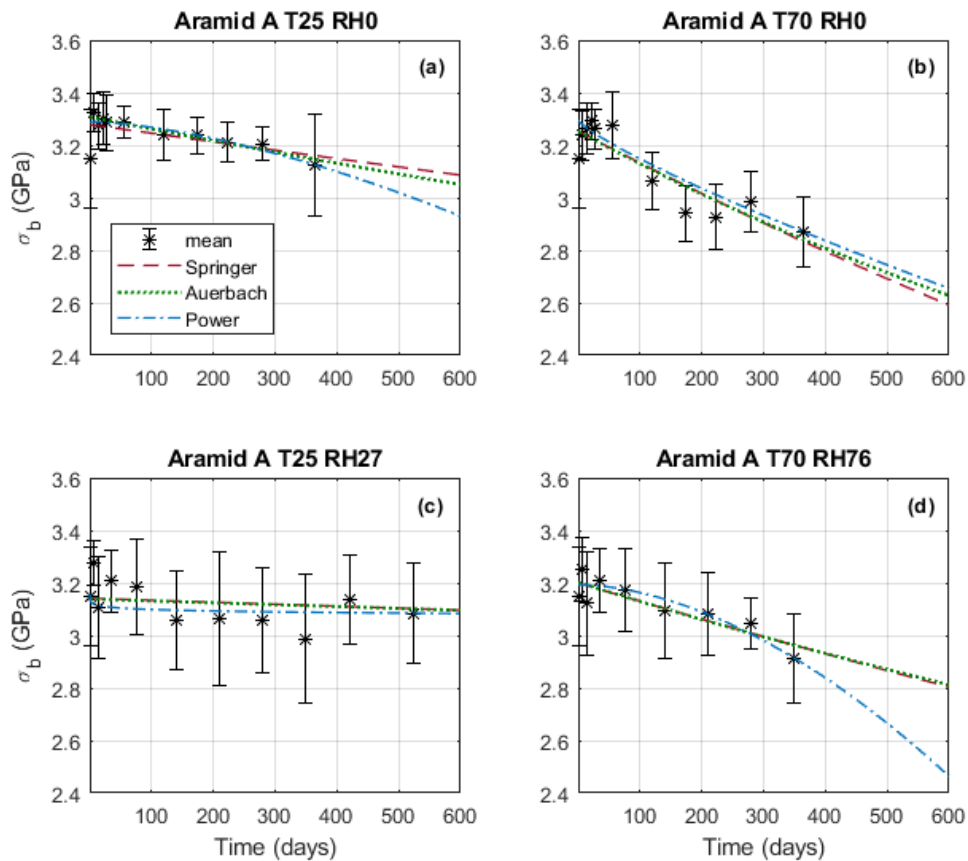


Figure 2. Representative results showing curve fitting for data from Aramid A exposed at (a) 25 °C, dry; (b) 70 °C, dry; (c) 25 °C, 27 % RH; (d) 70 °C, 76 % RH. Data points are the mean, error bars represent standard deviation.

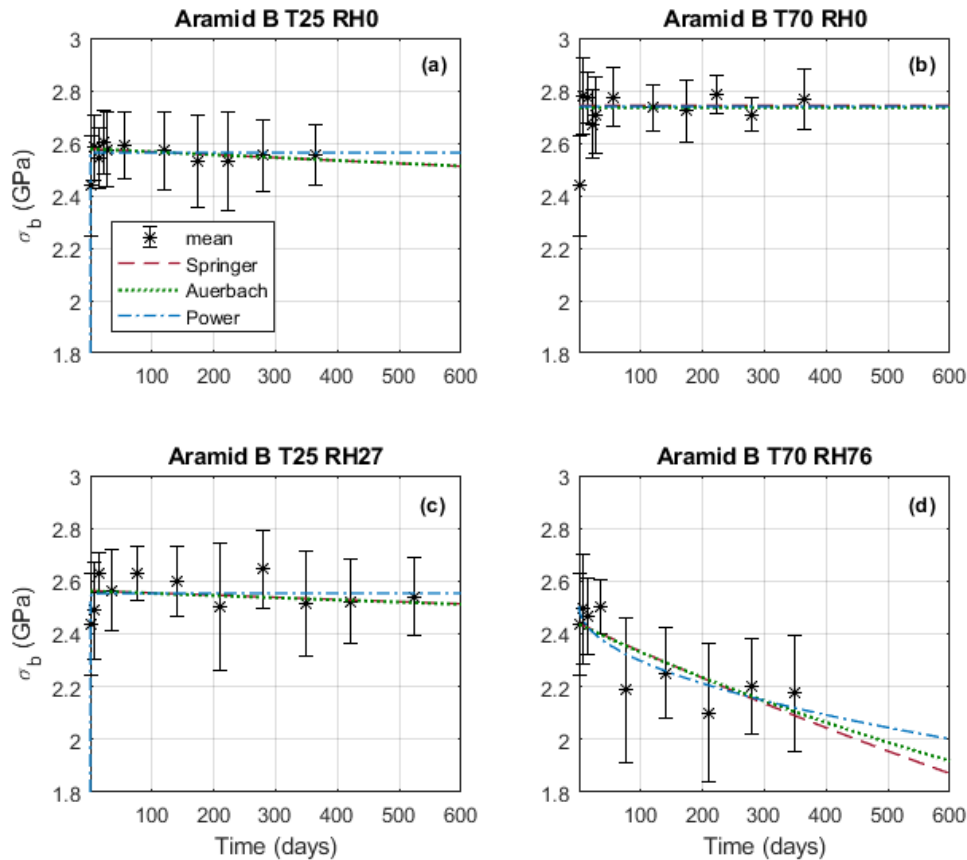


Figure 3. Representative results showing curve fitting for data from Aramid B exposed at (a) 25 °C, dry; (b) 70 °C, dry; (c) 25 °C, 27 % RH; (d) 70 °C, 76 % RH. Data points are the mean, error bars represent standard deviation.

Table 3. R-squared values for the three models compared at specified ageing conditions.

	Aramid A			Aramid B		
	Auerbach	Springer	Power-law	Auerbach	Springer	Power-law
25 °C, 0 % RH	0.7760	0.4178	0.7708	0.5307	0.2866	0.7136
25 °C, 27 % RH	0.7908	0.8157	0.7823	0.7333	0.5802	0.7987
70 °C, 0 % RH	0.0556	0.0589	0.0535	0.0956	0.0960	0.0619
70 °C, 76 % RH	0.7501	0.7875	0.8202	0.5563	0.6522	0.6815

The Springer model typically has a_1 approximately equal to one. In these cases, a single exponential decay process will fit the data almost as well as the Springer model. In addition, when a_1 is approximately equal to one it is harder to estimate the best fit parameters for the Springer model as two of the parameters have very little influence on the outcome.

All models perform similarly in fitting data for Aramid A at 25 °C, 27 % RH and 70 °C, dry, as shown by the r-squared values. In general, the models are in fairly good agreement for aramid A, particularly the power-law model and Auerbach's model. For aramid B the only condition with any degradation was the 70 °C, 76 % RH condition. For this condition the power-law model does seem to better explain the data. However, given the scatter in the data it is hard to derive much meaning from the relatively small differences in r-squared values.

As seen above in Table 1, there is very little evidence of any degradation for Aramid B for all conditions except 70 °C, 76 % RH. Aramid A again appears to degrade at both of the 70 °C conditions, but not at 25 °C, 27 % RH.

At 70 °C, 76 % RH aramid A retained 92.7 % of its initial strength, while aramid B retained 86.5 %. Since the failure strains were relatively invariant, Equation 6 can be used to provide a first-order estimate relating the change in ultimate tensile strength to a change in the expected V_{50} value of hypothetical armour constructed from these materials. The degradation in tensile strength leads to predicted decreases in V_{50} of 3.7 % for aramid A and 7.0 % for aramid B.

4. CONCLUSIONS AND FUTURE WORK

The analysis presented herein has shown that generally aramids are very stable and do not readily degrade at ambient or use conditions (near body temperature). After 350 days at continuous exposures of 70 °C, 76 % RH, aramid A retained nearly 93 % of its initial strength, and aramid B retained approximately 87 % of its initial strength. These conditions are much hotter and more humid than would be expected to be encountered by law enforcement officers, so these results should inspire confidence in the longevity of aramid-based armour systems. It should be noted however, that the aramid strength data have a broad distribution, and in future experiments, more replicates should be planned to better sample the distribution of strengths for this material.

An analysis of three different analytical models to predict degradation was conducted and broadly these models describe the data equally. A possible exception is the Springer model, which is more difficult to fit than the other two due to it having more parameters. For the 70 °C, 76 % RH condition, where there was some degradation, the power-law model was marginally better at describing the data for both aramids. Though degradation was also seen at 70 °C without humidity in aramid A, none of the models considered here provide a good description of this degradation.

Using the models presented herein, there is a predicted decrease of less than ten percent, under the extreme conditions of 70 °C, 76 % RH for one year, in V_{50} due to the strength degradation seen in this study. Further work will include a more detailed prediction of V_{50} , based not only on the strength degradation but also considering any changes in failure strain, density, or changes in the adjustment parameter θ .

Acknowledgments

The authors would like to thank John Jendzurski for assistance with the MATLAB data import, and Joannie Chin and S. Leigh Phoenix for helpful discussions.

References

- [1] A. L. Forster, P. Pintus, G. H. R. Messin, M. A. Riley, S. Petit, W. Rossiter, J. Chin, and K. D. Rice, "Hydrolytic stability of polybenzobisoxazole and polyterephthalamide body armor," *Polym. Degrad. Stab.*, vol. 96, no. 2, pp. 247–254, 2011.
- [2] J. Chin, E. Byrd, A. Forster, and P. Stutzman, "Chemical and Physical Characterization of Poly(p-phenylene-2,6-benzobisoxazole) Fibers Used in Body Armor Used in Body Armor," Gaithersburg, MD, 2006.
- [3] A. L. Forster, K. D. Rice, M. a Riley, G. H. R. Messin, S. Petit, C. Clerici, P. Pintus, G. Holmes, and J. Chin, "Development of Soft Armor Conditioning Protocols for NIJ Standard – 0101 . 06 : Analytical Results," pp. 1–44, 2009.
- [4] U.S. Department of Justice, "Ballistic Resistance of Body Armor," *NIJ Standard-0101.06*. 2008.
- [5] A. L. Forster, A. M. Forster, J. W. Chin, J. S. Peng, C. C. Lin, S. Petit, K. L. Kang, N. Paulter, M. A. Riley, K. D. Rice, and M. Al-Sheikhly, "Long-term stability of UHMWPE fibers," *Polym. Degrad. Stab.*, vol. 114, pp. 45–51, 2015.
- [6] D. Tompkins, "Body armor safety initiative: To protect and serve... better.," *NIJ J.*, no. 254, 2006.
- [7] "IACP/DUPONT™ KEVLAR® SURVIVORS' CLUB®." [Online]. Available: <http://www.dupont.com/products-and-services/personal-protective-equipment/body-armor/articles/the-kevlar-survivors-club.html>. [Accessed: 17-Jan-2017].

- [8] T. Bachner, "Rational Replacement Policy- A Recommendation to the Law Enforcement Community." 1985.
- [9] D. Frank, "Ballistic Tests of Used Soft Body Armor," *Natl. Bur. Stand. Interag. Rep. NBSIR 86-3444*, 1986.
- [10] C. Arrieta, É. David, P. Dolez, and T. Vu-Khanh, "Hydrolytic and photochemical aging studies of a Kevlar-PBI blend," *Polym. Degrad. Stab.*, vol. 96, no. 8, pp. 1411–1419, 2011.
- [11] G. Derombise, L. Vouyovitch Van Schoors, E. A. Klop, A. H. M. Schotman, G. Platret, and P. Davies, "Crystallite size evolution of aramid fibres aged in alkaline environments," *J. Mater. Sci.*, vol. 47, no. 5, pp. 2492–2500, 2012.
- [12] H. Springer, A. A. B. U. Obaid, A. B. Prabawa, and G. Hinrichsen, "Influence of Hydrolytic and Chemical Treatment on the Mechanical Properties of Aramid and Copolyaramid Fibers," *Text. Res. J.*, vol. 94, no. 1994, pp. 588–594, 1995.
- [13] I. Auerbach, "Kinetics for the tensile strength degradation of nylon and kevlar yarns," *J. Appl. Polym. Sci.*, vol. 37, no. 8, pp. 2213–2227, 1989.
- [14] R. J. Morgan and N. L. Butler, "Hydrolytic degradation mechanism of Kevlar 49 fibers when dissolved in sulfuric acid," *Polym. Bull.*, vol. 27, no. 6, pp. 689–696, 1992.
- [15] G. Derombise, L. V. Van Schoors, and P. Davies, "Degradation of Aramid Fibers Under Alkaline and Neutral Conditions: Relations Between the Chemical Characteristics and Mechanical Properties," *J. Appl. Polym. Sci.*, vol. 116, pp. 2504–2514, 2010.
- [16] C. Guangming, Y. Haihua, and W. Weidong, "Evaluation of light and thermal aging performance of aramid fabric," in *Textile bioengineering and informatics symposium proceedings*, 2008, pp. 321–325.
- [17] A. A. Obaid, S. Yarlagadda, and J. W. Gillespie, "Combined effects of kink bands and hygrothermal conditioning on tensile strength of polyarylate liquid crystal co-polymer and aramid fibers," *J. Compos. Mater.*, p. 21998315574754, 2015.
- [18] A. A. Obaid, J. M. Deitzel, J. W. Gillespie, and J. Q. Zheng, "The effects of environmental conditioning on tensile properties of high performance aramid fibers at near-ambient temperatures," *J. Compos. Mater.*, vol. 45, no. 11, pp. 1217–1231, 2011.
- [19] H. Zhang, J. Zhang, J. Chen, X. Hao, S. Wang, X. Feng, and Y. Guo, "Effects of solar UV irradiation on the tensile properties and structure of PPTA fiber," *Polym. Degrad. Stab.*, vol. 91, no. 11, pp. 2761–2767, Nov. 2006.
- [20] S. Bourbigot, X. Flambard, and F. Poutch, "Study of the thermal degradation of high performance fibres- application to polybenzole and p-aramid fibres," *Polym. Degrad. Stab.*, vol. 74, pp. 283–290, 2001.
- [21] P. M. Cuniff, "Dimensionless Parameters for Optimization of Textile-Based Armor Systems," in *18th International Symposium on Ballistics*, 1999, pp. 1302–1310.
- [22] S. Phoenix and P. Porwal, "A new membrane model for the ballistic impact response and V50 performance fo multi-ply fibrous systems.," *Int. J. Solids Struct.*, vol. 40, pp. 6723–6765, 2003.